Modification of magnetohydrodynamic waves by the relativistic Hall effect

Yohei Kawazura*

Rudolf Peierls Centre for Theoretical Physics, University of Oxford, Oxford OX1 3NP, United Kingdom

(Received 21 February 2017; revised manuscript received 15 May 2017; published 12 July 2017)

This study shows that a relativistic Hall effect significantly changes the properties of wave propagation by deriving a linear dispersion relation for relativistic Hall magnetohydrodynamics (HMHD). Whereas, in nonrelativistic HMHD, the phase and group velocities of fast magnetosonic wave become anisotropic with an increasing Hall effect, the relativistic Hall effect brings upper bounds to the anisotropies. The Alfvén wave group velocity with strong Hall effect also becomes less anisotropic than the nonrelativistic case. Moreover, the group velocity surfaces of Alfvén and fast waves coalesce into a single surface in the direction other than near perpendicular to the ambient magnetic field. It is also remarkable that a characteristic scale length of the relativistic HMHD depends on ion temperature, magnetic field strength, and density while the nonrelativistic HMHD scale length, i.e., ion skin depth, depends only on density. The modified characteristic scale length increases as the ion temperature increases and decreases as the magnetic field strength increases.

DOI: 10.1103/PhysRevE.96.013207

I. INTRODUCTION

Plasmas are multiscale in nature, meaning that macroscopic dynamics are influenced by microscopic effects. Although magnetohydrodynamics (MHD) is a simple and powerful model to capture "overall" dynamics in both space and laboratories (see, e.g., Refs. [1,2]), it fails to describe real phenomena when microscopic effects are not negligible. To solve this issue, MHD has been extended by including various microscopic effects [3–6]. As one of the primary extensions, Hall magnetohydrodynamics (HMHD) was proposed [4] and has been studied extensively in astrophysics, e.g., reconnection [7], accretion disks [8–10], dynamo [11,12], nonlinear Alfvén wave [13], and outflows [14], as well as in fusion [15,16].

When studying astrophysical objects, it is also essential to consider relativistic effects. Relativistic MHD [17,18] has been a *de facto* standard model for understanding large scale astrophysical phenomena. However, for the same reason as the nonrelativistic MHD, the lack of microscopic effects may be a critical shortcoming. Koide's extended version of the relativistic MHD (XMHD), in contrast, takes into account several microscopic effects originating from two-fluid nature [19,20]. This model has been highlighted in recent studies [21–24]

To understand these various MHD models, it is crucial to consider the properties of linear wave propagation. While the linear wave properties for nonrelativistic ideal MHD have been widely known (see Refs. [1,2]), the detailed analysis of HMHD waves was not conducted until Hameiri *et al.* revealed that phase and group diagrams are deformed by the Hall effect [25]. In addition to the nonrelativistic models, the dispersion relation for relativistic ideal MHD has been studied [17,18,26,27]. Keppens and Meliani drew phase and group diagrams of the relativistic MHD showing that there is no qualitative difference between nonrelativistic and relativistic diagrams in a fluid rest frame, except for the presence of the light limit [27]. In addition to the relativistic MHD, there are studies on wave properties for relativistic electron-positron pair plasma [28–30]. For relativistic electron-ion plasma, whereas the dispersion relation for the relativistic XMHD was derived by Koide [19] in specific wave vector configurations, a general dispersion relation in any wave vector direction has not been formulated. Hence the phase and group diagrams for the relativistic XMHD are unknown.

One might assume that relativistic HMHD diagrams are similar to the nonrelativistic HMHD diagrams, because the relativistic and the nonrelativistic MHD diagrams are similar. In this paper, we show that it is not true; we formulate the linear dispersion relation of the relativistic HMHD in any wave vector direction and show that, depending on whether the Hall effect is relativistic or nonrelativistic, there are differences in the way wave properties are changed.

II. DERIVATION OF RELATIVISTIC HMHD DISPERSION RELATION

Let us consider ion-electron plasma in Minkowski spacetime with a metric diag$(1,\,-1,\,-1,\,-1)$. We begin with relativistic XMHD [19,20] which contains electron rest mass and thermal inertial effects, the thermal electromotive effect, and the Hall effect. In this study, we focus on the Hall effect and ignore the other effects by assuming that the electron to ion mass ratio is zero and the electron temperature is at most on the order of the rest mass energy, i.e., $T_\mathrm{e}/m_\mathrm{e}c^2 \lesssim 1$ with electron's temperature T_e, rest mass m_e, and speed of light c. From the latter condition, we may neglect all the terms including electron's thermal enthalpy and pressure in the momentum equation and the generalized Ohm's law [31]. Thus we obtain the relativistic HMHD equations: the continuity equation,

$$\partial_\nu(nu^\nu) = 0, \tag{1}$$

the momentum equation,

$$\partial_\nu(nhu^\mu u^\nu) = \partial^\mu p + J_\nu F^{\mu\nu}, \tag{2}$$

the generalized Ohm's law,

$$enu_\nu F^{\mu\nu} - J_\nu F^{\mu\nu} = 0, \tag{3}$$

and the Maxwell's equations,

$$\partial_\mu F^{\mu\nu} = 4\pi J^\nu, \quad \partial^\mu(\epsilon_{\mu\nu\rho\sigma}F^{\rho\sigma}) = 0. \tag{4}$$

*yohei.kawazura@physics.ox.ac.uk

Multiplying u_μ by (2), the adiabatic equation is obtained,

$$\partial_\nu(\sigma u^\nu) = 0. \tag{5}$$

Here, e, n, h, p, and σ are elementary charge, rest frame number density, ion thermal enthalpy, ion thermal pressure, and ion entropy density, respectively. We have also defined the four-velocity $u^\mu = (\gamma, \gamma \mathbf{v}/c)$, the Faraday tensor $F^{\mu\nu}$, the four-current $J^\nu = \partial_\mu F^{\mu\nu} = (\rho_q, \mathbf{J}/c)$ where $\gamma = 1/\sqrt{1-(|\mathbf{v}|/c)^2}$ is the Lorentz factor, $\epsilon_{\mu\nu\rho\sigma}$ is the four-dimensional Levi-Civita symbol, and ρ_q is the charge density. The only difference between the relativistic ideal MHD is the second term in (3) which corresponds to a Hall term. The 3+1 decompositions of (1)–(5) are written as

$$\begin{aligned}
\partial_t(n\gamma) + \nabla\cdot(n\gamma\mathbf{v}) &= 0,\\
\partial_t(nh\gamma^2\mathbf{v}) + \nabla\cdot(nh\gamma^2\mathbf{v}\mathbf{v}) &= -c^2\nabla p + c^2\rho_q\mathbf{E}\\
&\quad + c\mathbf{J}\times\mathbf{B},\\
c(\gamma e n - \rho_q)\mathbf{E} + (\gamma e n\mathbf{v} - \mathbf{J})\times\mathbf{B} &= 0,\\
\partial_t(\sigma\gamma) + \nabla\cdot(\sigma\gamma\mathbf{v}) &= 0,\\
\nabla\cdot\mathbf{E} &= 4\pi\rho_q,\\
-\partial_t\mathbf{E} + c\nabla\times\mathbf{B} &= 4\pi\mathbf{J},\\
\nabla\cdot\mathbf{B} &= 0,\\
\partial_t\mathbf{B} + c\nabla\times\mathbf{E} &= 0,
\end{aligned}$$

with the electric field $\mathbf{E}$ and the magnetic field $\mathbf{B}$. Here, the time components of (2) and (3) are not shown since the former is dependent on the adiabatic equation (5), and the latter is dependent on the spatial component of the Ohm's law itself.

Next, we linearize these equations by separating the variables into homogeneous background fields denoted by subscripts 0 and small amplitude perturbations denoted by tilde symbols that are proportional to $\exp(i\mathbf{k}\cdot\mathbf{x} - \omega t)$ with the wave vector $\mathbf{k}$ and the frequency ω. We set the frame as the fluid rest frame by assuming $\mathbf{v}_0 = 0$ (the frame may be Lorentz transformed to the laboratory frame in the same manner as [27]). The background part of Maxwell's equations lead $\rho_{q0} = 0$, $\mathbf{E}_0 = 0$, and $\mathbf{J}_0 = 0$. In the following, we assume the ideal gas equation of state $h = mc^2 + [\Gamma/(\Gamma-1)]T$ where T is the ion temperature, and $\Gamma = 4/3$ is a specific heat ratio in ultrarelativistic case [32]. Then we get a set of equations that the perturbations satisfy,

$$-i\omega\tilde{n} + in_0\mathbf{k}\cdot\tilde{\mathbf{v}} = 0, \tag{6}$$

$$-i\omega n_0 h_0\tilde{\mathbf{v}} = -i\mathbf{k}c^2\tilde{p} + c\tilde{\mathbf{J}}\times\mathbf{B}_0, \tag{7}$$

$$\tilde{\mathbf{E}} + \frac{1}{c}\left(\tilde{\mathbf{v}} - \frac{\tilde{\mathbf{J}}}{en_0}\right)\times\mathbf{B}_0 = 0, \tag{8}$$

$$-i\omega\tilde{p} = -\frac{\Gamma p_0}{n_0}i\omega\tilde{n}, \tag{9}$$

$$\frac{4\pi}{c}\tilde{\mathbf{J}} = i\mathbf{k}\times\tilde{\mathbf{B}} + \frac{1}{c}i\omega\tilde{\mathbf{E}}, \tag{10}$$

$$i\mathbf{k}\cdot\tilde{\mathbf{B}} = 0, \tag{11}$$

$$i\mathbf{k}\times\tilde{\mathbf{E}} = \frac{1}{c}i\omega\tilde{\mathbf{B}}, \tag{12}$$

where h_0 is the backgroud part of h, and $p_0 = n_0T_0$ is the equilibrium ion pressure. We note that the previous study on the relativistic XMHD wave [19] assumed $\tilde{\rho}_q = 0$, which results in $\mathbf{k}\cdot\tilde{\mathbf{E}} = \mathbf{k}\cdot\tilde{\mathbf{J}} = 0$. Although this assumption makes the analysis simple (see Appendix B), it is not generally true. In the present study, we do not assume this condition. Below, we omit the tilde symbols.

Without loss of generality, one may assume $\mathbf{k} = (k_\perp, 0, k_{||})$ and $\mathbf{B}_0 = (0,0,B_0)$. We ignore the entropy mode, i.e., $\omega \neq 0$. Manipulating (6)–(12), we obtain the dispersion relation (see Appendix A for the detailed derivation).

$$\begin{aligned}
&\left(\omega^2 - k_{||}^2V_\mathrm{A}^2\right)\left\{\omega^4 - \left[k^2\left(V_\mathrm{A}^2 + \frac{n_0h_0}{\mathcal{M}}C_\mathrm{S}^2\right) + c^{-2}C_\mathrm{S}^2V_\mathrm{A}^2k_{||}^2\right]\right.\\
&\quad\left.\times\,\omega^2 + k^2k_{||}^2V_\mathrm{A}^2C_\mathrm{S}^2\right\}\\
&\quad = \delta_\mathrm{i}^2V_\mathrm{A}^2\omega^2c^{-4}\left(\omega^2 - k_{||}^2c^2\right)\left(\omega^2 - k^2c^2\right)\left(\omega^2 - k^2C_\mathrm{S}^2\right),
\end{aligned} \tag{13}$$

where

$$\begin{aligned}
&\mathcal{M} = n_0h_0 + \frac{B_0^2}{4\pi}, \quad \frac{C_\mathrm{S}}{c} = \sqrt{\frac{\Gamma p_0}{n_0h_0}},\\
&\frac{V_\mathrm{A}}{c} = \frac{B_0}{\sqrt{4\pi\mathcal{M}}},\ \delta_\mathrm{i}^2 = \frac{h_0^2}{4\pi\mathcal{M}e^2}
\end{aligned} \tag{14}$$

are total (fluid and magnetic) enthalpy [27], sound speed, Alfvén speed, and *modified* ion skin depth, respectively. We also have an identity $1 - V_\mathrm{A}^2/c^2 = n_0h_0/\mathcal{M}$. Taking the $\delta_\mathrm{i} \to 0$ limit, (13) becomes the relativistic ideal MHD dispersion relation [27]. In the nonrelativistic limit, δ_i becomes the familiar ion skin depth $d_\mathrm{i} = \sqrt{mc^2/4\pi n_0e^2}$. One finds that δ_i depends on both B_0 and T_0 as well as n_0. This is remarkably different from the nonrelativistic ion skin depth d_i which depends only on n_0. δ_i monotonically increases with increasing T_0 and monotonically decreases with increasing B_0. The T_0 dependence is straightforward, i.e., a high temperature induces large effective mass resulting in a long inertial length. This dependence has been pointed out in past studies [21,24,33]. However, the shrink of the inertial length by large B_0 is not trivial. Let us use $\beta = 8\pi n_0T_0/B_0^2$ and $\hat{T} = T_0/mc^2$ as parameters instead of T_0 and B_0. One may rewrite the modified ion skin depth as

$$\delta_\mathrm{i}^2 = d_\mathrm{i}^2\frac{\hat{h}^2}{\hat{h} + 2\hat{T}/\beta}, \tag{15}$$

where $\hat{h} = h_0/mc^2$. One finds that δ_i vanishes for small beta plasma. Therefore if the magnetic field is very strong, the plasma behaves like ideal MHD. One may interpret this as follows. The Alfvén speed is written as $V_\mathrm{A} = \Omega_\mathrm{c}\delta_\mathrm{i}$ where $\Omega_\mathrm{c} = ceB_0/h_0$ is the relativistic cyclotron frequency. When one takes the nonrelativistic limit (shown below), this becomes the familiar expression $V_\mathrm{A} = \Omega_\mathrm{c}d_\mathrm{i}$ with the nonrelativistic cyclotron frequency $\Omega_\mathrm{c} = eB_0/mc^2$. Whereas the cyclotron frequency is proportional to the magnetic field strength, the Alfvén speed may not exceed the speed of light [see (14)]; hence the modified skin depth is required to shrink as the magnetic field strength increases.

We note that the dispersion relation (13) and the modified inertial length δ_{i} are valid as long as the relativistic two-fluid equations are correct for ion-electron plasma since (1)–(5) are rigorously derived by the relativistic two-fluid equations [19,20]. However, it is proven that there are limitations for nonrelativistic HMHD dispersion relation when it is derived from a kinetic theory [34,35]. It is a open question whether the dispersion relation (13) is derived from the relativistic kinetic theory.

Next let us consider the nonrelativistic limit,

$$h_0 \to mc^2,\ \mathcal{M} \to n_0 mc^2,\ \frac{\omega^2}{c^2 k_{||}^2} \to 0,\ \frac{\omega^2}{c^2 k^2} \to 0. \tag{16}$$

We get $\delta_{\mathrm{i}} \to d_{\mathrm{i}}$, $(V_{\mathrm{A}}/c)^2 \to 2\hat{T}/\beta$, and $(C_{\mathrm{S}}/c)^2 \to \Gamma\hat{T}$. Then (13) yields nonrelativistic HMHD dispersion relation [25],

$$\begin{aligned}&\left(\omega^2 - k_{||}^2 V_{\mathrm{A}}^2\right)\left\{\omega^4 - k^2\left(V_{\mathrm{A}}^2 + C_{\mathrm{S}}^2\right)\omega^2 + k^2 k_{||}^2 V_{\mathrm{A}}^2 C_{\mathrm{S}}^2\right\}\\ &\quad = d_{\mathrm{i}}^2 V_{\mathrm{A}}^2 \omega^2 k_{||}^2 k^2\left(\omega^2 - k^2 C_{\mathrm{S}}^2\right).\end{aligned} \tag{17}$$

Since in the nonrelativistic case, $C_{\mathrm{S}}/V_{\mathrm{A}}$ does not depend on $\hat{T}$, the shape of the phase and group diagrams are independent of $\hat{T}$ [1].

III. ANALYSIS OF RELATIVISTIC HMHD DISPERSION RELATION

In the beginning, we show two apparent differences between the relativistic dispersion relation (13) and the nonrelativistic one (17). First, for exactly perpendicular propagation, viz., $k_{||} = 0$, the right-hand side of (13) is finite whereas the right-hand side of (17) vanishes. Therefore, for this direction, the nonrelativistic Hall effect does not change the wave properties [25], but the relativistic Hall effect does. Second, the right-hand side of (13) is quartic with respect to ω^2 while the left hand is cubic. This means that the relativistic HMHD has one additional wave solution that neither appears in relativistic ideal MHD nor nonrelativistic HMHD [the right-hand side of (17) is quadratic]. As we show below, this extra wave is superluminous which becomes light wave at infinitely large $k\delta_i$. The other three waves are shear Alfvén wave, and slow and fast magnetosonic waves. Below, for notational brevity, superscripts A, F, and S denote the Alfvén, fast, and slow waves, respectively.

Let us start by the analysis in $k_{||} = 0$ direction. Again, the nonrelativistic dispersion relation (17) becomes ideal MHD in this direction. The relativistic dispersion relation (13) becomes the quadratic equation. The solutions are analytically obtained as

$$\left(v_{\mathrm{ph}}^{\pm}\right)^2 = \frac{1}{2}\left\{1 + \hat{C}_{\mathrm{S}}^2 + \frac{1}{(k_\perp\delta_{\mathrm{i}})^2\hat{V}_{\mathrm{A}}^2} \pm \sqrt{\left[1 + \hat{C}_{\mathrm{S}}^2 + \frac{1}{(k_\perp\delta_{\mathrm{i}})^2\hat{V}_{\mathrm{A}}^2}\right]^2 - 4\left[\hat{C}_{\mathrm{S}}^2 + \frac{1}{(k_\perp\delta_{\mathrm{i}})^2\hat{V}_{\mathrm{A}}^2}\left(\hat{V}_{\mathrm{A}}^2 + \frac{n_0 h_0}{\mathcal{M}}C_{\mathrm{S}}^2\right)\right]}\right\}, \tag{18}$$

where $\mathbf{v}_{\mathrm{ph}} = (v_{\mathrm{ph}\perp}, 0, v_{\mathrm{ph}||}) = (\omega/ck)\,\mathbf{n}$ is the normalized phase velocity with $\mathbf{n} = \mathbf{k}/k$, and $\hat{V}_{\mathrm{A}} = V_{\mathrm{A}}/c$ and $\hat{C}_{\mathrm{S}} = C_{\mathrm{S}}/c$ which are normalized Alfvén and sound speed. One may show that v_{ph}^+ (v_{ph}^-) is always larger (smaller) than unity. Thus v_{ph}^+ is the superluminous wave. These two solutions become $(v_{\mathrm{ph}}^+)^2 \to 1$ and $(v_{\mathrm{ph}}^-)^2 \to \hat{C}_{\mathrm{S}}^2$ for the $k_\perp\delta_{\mathrm{i}} \to \infty$ limit, and $(v_{\mathrm{ph}}^+)^2 \to \infty$ and $(v_{\mathrm{ph}}^-)^2 \to \hat{V}_{\mathrm{A}}^2 + \hat{C}_{\mathrm{S}}^2(n_0 h_0/\mathcal{M}) = \hat{C}_{\mathrm{S}}^2 + (1 - \hat{C}_{\mathrm{S}}^2)\hat{V}_{\mathrm{A}}^2$ (which is the fast wave phase speed for the ideal MHD) for the $k\delta_{\mathrm{i}} \to 0$ limit. The behavior of the superluminous solution is the same as the ordinary wave in the strongly magnetized relativistic electron-positron plasma [36,37]. The disappeared two solutions become the shear Alfvén and the slow waves in the $k_{||} \neq 0$ direction.

Next we consider rough dependence of phase speed on $k\delta_{\mathrm{i}}$ when the magnitude of $k\delta_{\mathrm{i}}$ is large. As shown in Ref. [25] for the nonrelativistic case, the phase speed of the three HMHD waves are $v_{\mathrm{ph}}^{\mathrm{F}} \sim O((kd_{\mathrm{i}})^2)$, $v_{\mathrm{ph}}^{\mathrm{S}} \sim O(1/(kd_{\mathrm{i}})^2)$, and $v_{\mathrm{ph}}^{\mathrm{A}} \sim O(1/(kd_{\mathrm{i}})^2)$, respectively; since the left-hand side in (17) is $\sim v_{\mathrm{ph}}^6$ and the right-hand side is $\sim (kd_{\mathrm{i}})^2 v_{\mathrm{ph}}^4$, the solution with $O((kd_{\mathrm{i}})^2)$ exists. Thus, $v_{\mathrm{ph}}^{\mathrm{F}}$ increases as kd_{i} increases. On the other hand for the relativistic case (13), the left-hand side is $\sim v_{\mathrm{ph}}^6$ and the right-hand side is $\sim (k\delta_{\mathrm{i}})^2 v_{\mathrm{ph}}^8$. Therefore, a solution with $O((k\delta_{\mathrm{i}})^2)$ does not exist, and the phase speed of the all wave may not increase as $k\delta_{\mathrm{i}}$ increases. This fact is reasonable for the fast, slow, and Alfvén waves because their phase speed may not exceed c. In the $k_{||} = 0$ direction, this is exactly confirmed by (18) which is principally $O(1/(k_\perp\delta_{\mathrm{i}})^2)$ and decreases monotonically.

As shown in Ref. [25], in the nonrelativistic case, $v_{\mathrm{ph}}^{\mathrm{F}}$ increases except in the $k_{||} = 0$ direction as kd_{i} increases. Since the diagram for the ideal MHD fast wave is a circular shape, it becomes a dumbbell shape stretched in the parallel direction at large kd_{i}. On the other hand, in the relativistic case, $v_{\mathrm{ph}}^{\mathrm{F}}$ may not increase; especially in the $k_{||} = 0$ direction, $(v_{\mathrm{ph}}^{\mathrm{F}})^2$ decreases from $\hat{C}_{\mathrm{S}}^2 + (1 - \hat{C}_{\mathrm{S}}^2)\hat{V}_{\mathrm{A}}^2$ to $\hat{C}_{\mathrm{S}}^2$ as $k\delta_{\mathrm{i}}$ increases. Therefore the resulting phase diagram at large $k\delta_{\mathrm{i}}$ is less anisotropic than the nonrelativistic phase diagram.

Next we consider the aforementioned nonrelativistic limit more carefully. There are two relativistic effects included, the ion thermal inertia effect and the displacement current. The former effect is eliminated by assuming $\hat{T} \ll 1$, which results in $h_0 \to mc^2$. The situation is divided in two cases depending on the value of $\hat{T}/\beta$ since $\mathcal{M} \to n_0 mc^2(1 + 2\hat{T}/\beta)$. For a moderately or weakly magnetized case, we get $\mathcal{M} \to n_0 mc^2$ which results in $\delta_{\mathrm{i}} \to d_{\mathrm{i}}$. Therefore the change of the inertial length does not happen. For a strongly magnetized case, we get $\delta_{\mathrm{i}}^2 \to d_{\mathrm{i}}^2/(1 + 2\hat{T}/\beta)$; thus the inertial length may change, and the change is due to the displacement current. In both cases, the structure of the dispersion relation does not change from (13). Therefore, the superluminous solution still exists, and the phase speed for all waves is $O(1/(k\delta_{\mathrm{i}})^2)$.

The other relativistic effect, displacement current, is eliminated by taking $\mathcal{M} \to n_0 mc^2$, $\omega^2/c^2 k_{||}^2 \to 0$, and $\omega^2/c^2 k^2 \to$

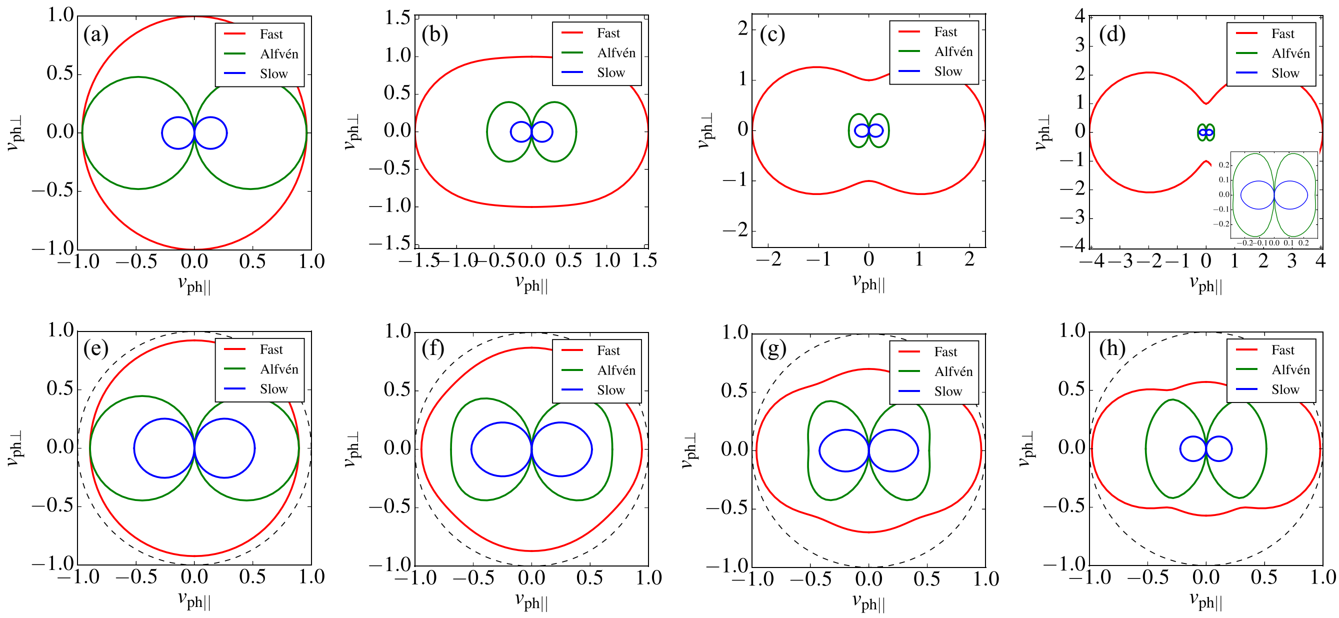

FIG. 1. The phase diagram for (a) nonrelativistic ideal MHD, (b)–(d) nonrelativistic HMHD, (e) relativistic ideal MHD, and (f)–(h) relativistic HMHD. β and $\hat{T}$ are fixed at 0.1 and 1.0, and kd_{i} varies as (0.0,1.0,2.0,4.0) from left to right panels. The vertical and horizontal axes in (a)–(d) are normalized by $v_{\mathrm{ph}}^{\mathrm{F}}$ with $kd_{\mathrm{i}}=0$ and $\theta=0$. The inset figure in (d) is an enlargement near the Alfvén wave. The red, green, and blue curves indicate the fast, Alfvén, and the slow modes, respectively. The broken circles indicate the light speed.

0. Accordingly we get $\delta_{\mathrm{i}}\to d_{\mathrm{i}}$, $(V_{\mathrm{A}}/c)^2\to 2\hat{T}/\beta$, and $(C_{\mathrm{S}}/c)^2\to\Gamma\hat{T}$. Obviously, this limit prohibits the superluminous solution; in fact, the right-hand side of (17) is ω^4. Since the order of the right-hand side has been lowered, phase speed with $O((k\delta_{\mathrm{i}})^2)$ is allowed. This solution is a nonrelativistic fast wave.

In summary, among the two relativistic effects, the ion thermal inertia only contributes to the change of the inertial length, and the displacement current contributes to the emergence of the superluminous solution and the wave dependence on $k\delta_{\mathrm{i}}$. As we show in the next section, this relativistic wave dependence on $k\delta_{\mathrm{i}}$ caused by the displacement current changes the phase and group diagrams dramatically.

Next we graphically show the phase diagram for the specific plasma parameter. For a given β, $\hat{T}$, and kd_{i}, the phase velocity $\mathbf{v}_{\mathrm{ph}}$ is determined as a function of $\theta=\cos^{-1}(k_{||}/k)$ by solving (13). Both C_{S}/c and V_{A}/c are monotonically increasing functions of $\hat{T}$ with upper bounds of $\sqrt{\Gamma-1}$ and $\sqrt{2(\Gamma-1)/[\beta\Gamma+2(\Gamma-1)]}$, respectively. Since C_{S} and V_{A} almost become the upper bound values for $\hat{T}\gtrsim 1$, we consider only a $\hat{T}=1$ case. Since the relativistic Hall effect disappears in very low beta plasmas as mentioned above, we consider the $\beta=0.1$ case. Such plasma parameters are relevant to Poynting flux dominated gamma ray bursts (see, for example, [38]). These settings yield $\delta_{\mathrm{i}}/d_{\mathrm{i}}=1$.

Figure 1 shows the phase diagrams with various $kd_{\mathrm{i}}=(0,0.5,1.0,4.0)$ for Figs. 1(a)–1(d) nonrelativistic and Figs. 1(e)–1(h) relativistic cases. For the nonrelativistic cases, the shape of the diagram is independent from $\hat{T}$, hence $\mathbf{v}_{\mathrm{ph}}$ is normalized by $v_{\mathrm{ph}}^{\mathrm{F}}$ at $\theta=\pi/2$, which is the same for any d_{i}. The nonrelativistic diagrams Figs. 1(a)–1(d) are the same as those in Ref. [25]. We find the phase speed of the fast wave ($v_{\mathrm{ph}}^{\mathrm{F}}$) increases with increasing kd_{i} except in the $\theta=\pi/2$ direction, hence the circular shaped phase velocity surface for $kd_{\mathrm{i}}=0$ [Fig. 1(a)] becomes elliptic [Fig. 1(c)] and finally dumbbell-like in shape [Fig. 1(d)]. This means that the fast wave becomes anisotropic in small scale. Another observation is that the phase speeds of the Alfvén wave ($v_{\mathrm{ph}}^{\mathrm{A}}$) and slow wave ($v_{\mathrm{ph}}^{\mathrm{S}}$) decrease with increasing kd_{i}. Thus, the fast wave gets separated from the other two waves. This separation is appreciable especially in the parallel direction.

Let us compare these results with the relativistic HMHD diagrams [Figs. 1(e)–1(h)]. Whereas the relativistic ideal MHD diagram [Fig. 1(e)] is qualitatively the same as the nonrelativistic ideal MHD one [Fig. 1(a)], the relativistic HMHD diagrams [Figs. 1(f)–1(h)] are significantly different from those of the nonrelativistic HMHD [Figs. 1(b)–1(d)]. The anisotropy of the fast wave is moderated so that the shape of the phase velocity surface does not become a dumbbell shape. This isotropization is explained as follows. In nonrelativistic HMHD, the anisotropy is created by the selective increase in $v_{\mathrm{ph}||}^{\mathrm{F}}$ as kd_{i}

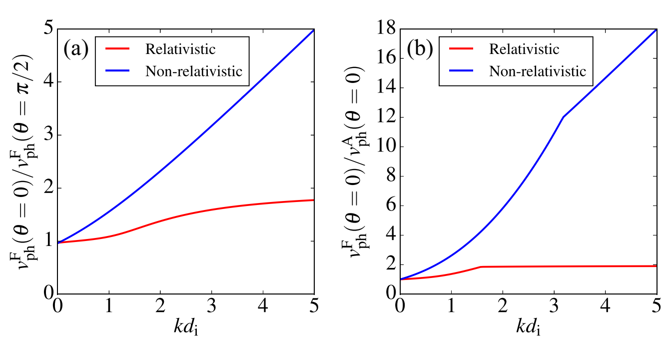

FIG. 2. (a) The anisotropy of the fast wave phase velocity and (b) the ratio of the fast phase speed to the Alfvén phase speed at $\theta=0$. The red and blue curves indicate the relativistic and the nonrelativistic cases, respectively. β and $\hat{T}$ are fixed at 0.1 and 1.0.

increases. In relativistic HMHD, on the other hand, $v_{\rm ph}^{\rm F}$ may not exceed the light limit, hence there is no room for the significant increase in $v_{\rm ph||}^{\rm F}$. Meanwhile, Figs. 1(e)–1(h) show that $v_{\rm ph\perp}^{\rm F}$ decreases as $kd_{\rm i}$ increases (recall that $v_{\rm ph\perp}^{\rm F}$ at $\theta = \pi/2$ is changeable for increasing $kd_{\rm i}$ unlike nonrelativistic HMHD). However, $v_{\rm ph\perp}^{\rm F}$ will eventually reach $v_{\rm ph\perp}^{\rm A}$ because $v_{\rm ph\perp}^{\rm A}$ does not decrease. Since $v_{\rm ph\perp}^{\rm F}$ may not be smaller than $v_{\rm ph\perp}^{\rm A}$, the decrease in $v_{\rm ph\perp}^{\rm F}$ is saturated at some value of $kd_{\rm i}$. In short, $v_{\rm ph}^{\rm F}$ is bounded from above by the light limit and from below by $v_{\rm ph}^{\rm A}$. Thus the anisotropy will stop increasing at some $kd_{\rm i}$.

Figure 2 explicitly illustrates this scenario. Figure 2(a) shows a measure of the fast wave anisotropy defined by $v_{\rm ph}^{\rm F}(\theta = 0)/v_{\rm ph}^{\rm F}(\theta = \pi/2)$ as a function of $kd_{\rm i}$ for the nonrelativistic and relativistic cases. One finds that the anisotropy increases almost linearly in the nonrelativistic case whereas it is bounded by ~ 2 in the relativistic case. Figure 2(b) shows the ratio of the fast phase speed to the Alfvén phase speed at $\theta = 0$. While, in the nonrelativistic case, the difference between the two speeds increases endlessly, the fast wave phase speed becomes at most twice as fast as the Alfvén phase speed for $kd_{\rm i} \gtrsim 1.5$ in the relativistic case. For the relativistic case, since the maximum of $v_{\rm ph\perp}^{\rm A}$ is almost the same as $v_{\rm ph}^{\rm A}(\theta = 0)$ for large $kd_{\rm i}$ [see Fig. 1(h)], the lower bound of $v_{\rm ph\perp}^{\rm F}$ is almost the same as $v_{\rm ph}^{\rm A}(\theta = 0)$. Therefore $v_{\rm ph}^{\rm F}(\theta = 0)/v_{\rm ph}^{\rm A}(\theta = 0) \sim 2$ corresponds to the fast wave anisotropy of ~ 2.

Next we consider a normalized group velocity $\mathbf{v}_{\rm gr} = (v_{\rm gr\perp}, 0, v_{\rm gr||}) = c^{-1}\partial\omega/\partial\mathbf{k}$; see Appendix C for full expression. Figure 3 shows the group diagrams for Figs. 3(a)–3(d) nonrelativistic and Figs. 3(e)–3(h) relativistic cases with the same parameters as Fig. 1. The nonrelativistic diagrams Figs. 3(a)–3(d) are the same as those in Ref. [25]. Here, we again find that there is no qualitative difference between relativistic ideal MHD [Fig. 3(e)] and nonrelativistic ideal MHD [Fig. 3(a)]. On the other hand, the relativistic HMHD diagrams [Figs. 3(f)–3(h)] are significantly different from those of the nonrelativistic HMHD [Figs. 3(b)–3(d)]. In the nonrelativistic case, the behavior of the fast wave group velocity ($\mathbf{v}_{\rm gr}^{\rm F}$) is similar to that of phase velocity; in the beginning, the group velocity surface is circular, then it becomes elliptic and successively dumbbell-like as $kd_{\rm i}$ increases. Since Alfvén wave becomes dispersive when the Hall effect is present, its group velocity becomes a triangle. We find that the Alfvén group velocity surface becomes acute-angled triangle at large $kd_{\rm i}$ [see the inset of Fig. 3(d)].

Let us compare these behaviors with the relativistic HMHD [Figs. 3(f)–3(h)]. We find that the fast and Alfvén group velocity surfaces coalesce into a single surface at large $kd_{\rm i}$. In the relativistic case, $v_{\rm gr||}^{\rm F}$ and $v_{\rm gr||}^{\rm A}$ is not allowed to increase as $kd_{\rm i}$ increases since they are almost at the light limit for $kd_{\rm i} = 0$ [Fig. 3(e)]. On the other hand, $v_{\rm gr\perp}^{\rm F}$ decreases as $kd_{\rm i}$ increases. Thus, the fast wave group velocity surface tends to be elliptic (Figs. 3(e)–3(g)]. Meanwhile, $v_{\rm gr\perp}^{\rm A}$ increases as $kd_{\rm i}$ increases [Figs. 3(e)–3(g)]. At some point, the increasing $v_{\rm gr\perp}^{\rm A}$ becomes the same value as the decreasing $v_{\rm gr\perp}^{\rm F}$. Thus the coalesce of the fast and Alfvén waves is realized. Since the fast wave speed may not be smaller than the Alfvén wave speed, the fast wave diagram no longer becomes dumbbell-like in shape. The Alfvén wave diagram also becomes less anisotropic since only $v_{\rm gr\perp}^{\rm A}$ increases as $kd_{\rm i}$ increases.

Figure 4(a) shows a measure of the fast wave anisotropy defined by $v_{\rm gr}^{\rm F}(\theta = 0)/v_{\rm gr}^{\rm F}(\theta = \pi/2)$ as a function of $kd_{\rm i}$ for the nonrelativistic and relativistic cases. One finds that the anisotropy linearly increases in the nonrelativistic case while it saturates at ~ 2 in the relativistic case. Figure 4(b) shows

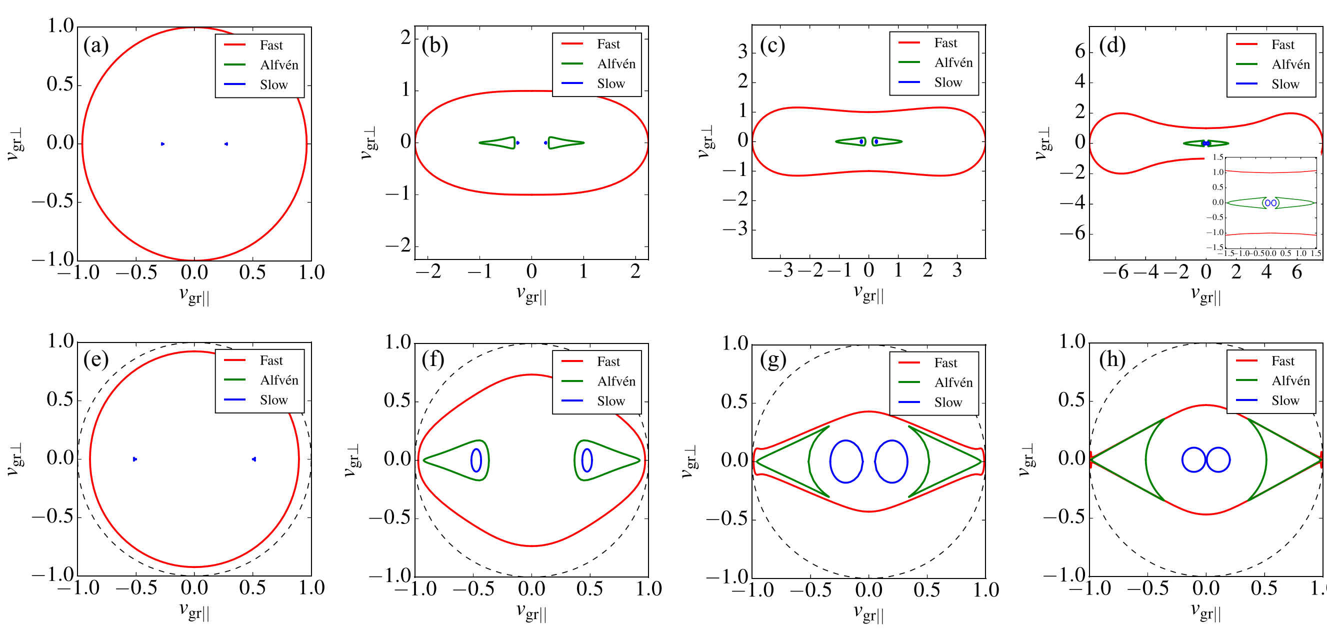

FIG. 3. The group diagram for (a) nonrelativistic ideal MHD, (b)–(d) nonrelativistic HMHD, (e) relativistic ideal MHD, and (f)–(h) relativistic HMHD. β and $\hat{T}$ are fixed at 0.1 and 1.0, and $kd_{\rm i}$ varies as (0.0,1.0,2.0,4.0) from left to right panels. The vertical and horizontal axes in (a)–(d) are normalized by $v_{\rm gr}^{\rm F}$ with $kd_{\rm i} = 0$ and $\theta = 0$. The inset figure in (d) is an enlargement near the Alfvén wave. The broken circles indicate the light speed.

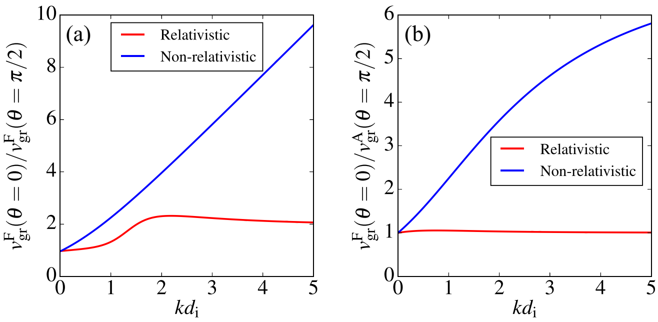

FIG. 4. (a) The anisotropy of the fast wave group velocity and (b) the ratio of the fast group speed at $\theta = 0$ to the Alfvén group speed at $\theta = \pi/2$. The red and blue curves indicate the relativistic and the nonrelativistic cases, respectively. β and $\hat{T}$ are at fixed at 0.1 and 1.0.

the ratio of the maximum of $v_{\rm gr}^{\rm F}$ to the maximum of $v_{\rm gr}^{\rm A}$, i.e., $v_{\rm gr}^{\rm F}(\theta=0)/v_{\rm gr}^{\rm A}(\theta=\pi/2)$. Here, $v_{\rm gr}^{\rm A}(\theta=\pi/2)$ corresponds to the vertex of the Alfvén surface on the $v_{\rm gr\perp}$ axis. Whereas the fast and Alfvén waves separate in the nonrelativistic case, such a separation is prohibited in the relativistic case.

IV. CONCLUSIONS

We have shown that the relativistic Hall effect changes the MHD wave properties in a different way from the nonrelativistic Hall effect; namely, *isotropization* and *coalescence* of the fast and shear Alfvén waves. It is also remarkable that the characteristic scale length $\delta_{\rm i}$ depends on ion temperature, magnetic field strength as well as density. This is different from the nonrelativistic ion skin depth $d_{\rm i}$ which depends only on density. The modified ion inertial length increases as the ion temperature increases whereas it decreases as the magnetic field strength increases. Therefore the Hall effect disappears, and plasma behaves like ideal MHD in very strong magnetic field.

ACKNOWLEDGMENTS

This work was supported by STFC Grant No. ST/N000919/1 and JSPS KAKENHI Grant No. 26800279.

APPENDIX A: DERIVATION OF (13)

In this section, we explicitly derive the relativistic HMHD dispersion relation (13). From (6) and (9), we get

$$p = \frac{n_0 h_0}{\omega}\frac{C_{\rm S}^2}{c^2}(\mathbf{k}\cdot\mathbf{v}).$$

Substituting this into (7), we get

$$-\omega n_0 h_0 \mathbf{v} = -\frac{n_0 h_0}{\omega} C_{\rm S}^2(\mathbf{k}\cdot\mathbf{v})\mathbf{k} + \frac{c}{i}\mathbf{J}\times\mathbf{B}_0. \tag{A1}$$

$\mathbf{k}\times$ (8) yields

$$\omega\mathbf{B} + k_{||}B_0\mathbf{v} - (\mathbf{k}\cdot\mathbf{v})\mathbf{B}_0 - \frac{1}{en_0}\big[k_{||}B_0\mathbf{J} - (\mathbf{k}\cdot\mathbf{J})\mathbf{B}_0\big] = 0. \tag{A2}$$

$\mathbf{k}\cdot$ (10) yields

$$\mathbf{k}\cdot\mathbf{J} = \frac{B_0}{4\pi c}i\omega\left[-(\mathbf{k}\times\mathbf{v})\cdot\hat{\mathbf{z}} + \frac{i}{4\pi en_0 c}(\omega^2 - c^2k^2)B_z\right]. \tag{A3}$$

$\mathbf{k}\cdot$ (A1) is manipulated using (10) and (12) as

$$\mathbf{k}\cdot\mathbf{v} = -\frac{B_0\omega(\omega^2 - c^2k^2)B_z}{4\pi n_0 h_0\big(\omega^2 - C_{\rm S}^2k^2\big)}. \tag{A4}$$

Eliminating v_z from the z components of (A1) and (A2) and using (A4), we get

$$\frac{\omega}{k_{||}B_0}B_z = -\frac{\omega^2 - C_{\rm S}^2k_{||}^2}{\omega k_{||}}\frac{B_0(\omega^2 - c^2k^2)B_z}{4\pi n_0 h_0\big(\omega^2 - C_{\rm S}^2k^2\big)} + \frac{1}{en_0}\left(J_z - \frac{\mathbf{k}\cdot\mathbf{J}}{k_{||}}\right). \tag{A5}$$

Substituting (A3) into $(\mathbf{k}\times$ (A1)$)\cdot\hat{\mathbf{z}}$, we get

$$(\mathbf{k}\times\mathbf{v})\cdot\hat{\mathbf{z}} = i\frac{cB_0}{\omega\mathcal{M}}\left[k_{||}J_z + \frac{B_0\omega}{(4\pi c)^2 en_0}(\omega^2 - c^2k^2)B_z\right]. \tag{A6}$$

Then we back-substitute this into (A3) to get

$$\mathbf{k}\cdot\mathbf{J} = \frac{V_{\rm A}^2}{c^2}k_{||}J_z + \left(\frac{V_{\rm A}^2}{c^2} - 1\right)\frac{\omega(\omega^2 - c^2k^2)B_0B_z}{(4\pi c)^2 en_0}. \tag{A7}$$

Next we substitute (A6) and (A7) into $(\mathbf{k}\times$ (A2)$)\cdot\hat{\mathbf{z}}$ to get

$$\begin{aligned}&\left[\frac{4\pi V_{\rm A}^2}{c}\omega k_{||}^2 - 4\pi c\omega k^2 - \frac{cB_0^2}{\omega\mathcal{M}}k_{||}^2(\omega^2 - c^2k^2)\right]J_z \\ &= \left[-\left(\frac{V_{\rm A}^2}{c^2} - 1\right)\frac{\omega^2 k_{||}(\omega^2 - c^2k^2)B_0}{4\pi cen_0} + \frac{B_0^3}{(4\pi)^2 cen_0\mathcal{M}}k_{||}(\omega^2 - c^2k^2)^2 - \frac{k_{||}B_0}{4\pi n_0 ce}(\omega^2 - c^2k^2)^2\right]B_z.\end{aligned} \tag{A8}$$

Substituting (A7) into (A5), we get

$$-\frac{1}{en_0}\left(\frac{V_{\rm A}^2}{c^2} - 1\right)J_z = \left[\frac{\omega}{k_{||}B_0} + \frac{B_0}{4\pi n_0 h_0}\frac{(\omega^2 - C_{\rm S}^2k_{||}^2)(\omega^2 - c^2k^2)}{\omega k_{||}\big(\omega^2 - C_{\rm S}^2k^2\big)} + \left(\frac{V_{\rm A}^2}{c^2} - 1\right)\frac{\omega(\omega^2 - c^2k^2)B_0}{(4\pi cen_0)^2 k_{||}}\right]B_z. \tag{A9}$$

Finally, we obtain the dispersion relation (13) by eliminating J_z from (A8) and (A9).

APPENDIX B: REDUCTION TO THE DISPERSION RELATION IN REF. [19]

In Ref. [19] the dispersion relation for XMHD is derived in the specific condition. The wave vector and the perturbed velocity are set in the configuration $\mathbf{k} = k_x\hat{\mathbf{x}}$ and $\mathbf{v} = v_x\hat{\mathbf{x}}$. Furthermore, the rather restrictive condition $\mathbf{k}\cdot\mathbf{E} = \mathbf{k}\cdot\mathbf{J} = 0$, which is led by the assumption $\rho_q = 0$, is imposed. Under these conditions, we may simplify (A1) and (A2) as

$$-\omega n_0 h_0 v_x = -\frac{n_0 h_0}{\omega} C_{\mathrm{S}}^2 k_x^2 v_x + \frac{c}{i} J_y B_0, \tag{B1}$$

and

$$\omega B_z - k_x v_x B_0 = 0. \tag{B2}$$

Combining with (10) and (12), we obtain the very simplified dispersion relation,

$$\omega^2 = \frac{4\pi n_0 h_0 C_{\mathrm{S}}^2 + c^2 B_0^2}{4\pi n_0 h_0 + B_0^2} k_\perp^2. \tag{B3}$$

This is the dispersion relation for the fast wave in Ref. [19].

APPENDIX C: GROUP VELOCITY

In a similar manner to Ref. [25], straightforward algebraic manipulation of (13) yields

$$\mathbf{v}_{\mathrm{gr}} = \frac{\mathbf{K} + (k\delta_{\mathrm{i}})^2\mathbf{L}}{M + (k\delta_{\mathrm{i}})^2 N}, \tag{C1}$$

with

$$\begin{aligned}
\mathbf{K} &= \left\{\left(\hat{V}_{\mathrm{A}}^2 + \frac{n_0 h_0}{\mathcal{M}}\hat{C}_{\mathrm{S}}^2\right)v_{\mathrm{ph}}^4 - \left[\hat{V}_{\mathrm{A}}^2 + \left(1 + \frac{n_0 h_0}{\mathcal{M}}\right)\hat{C}_{\mathrm{S}}^2\right]\hat{V}_{\mathrm{A}}^2\left(\frac{k_{||}}{k}\right)^2 v_{\mathrm{ph}}^2 + \hat{C}_{\mathrm{S}}^2\hat{V}_{\mathrm{A}}^4\left(\frac{k_{||}}{k}\right)^4\right\}\mathbf{n} \\
&\quad + \left\{(1+\hat{C}_{\mathrm{S}}^2)\hat{V}_{\mathrm{A}}^2\left(\frac{k_{||}}{k}\right)v_{\mathrm{ph}}^4 - \left[2\left(\frac{k_{||}}{k}\right)^2\hat{V}_{\mathrm{A}}^2\hat{C}_{\mathrm{S}}^2 + \left[\hat{V}_{\mathrm{A}}^2 + \left(1 + \frac{n_0 h_0}{\mathcal{M}}\right)\hat{C}_{\mathrm{S}}^2\right]\right]\hat{V}_{\mathrm{A}}^2\left(\frac{k_{||}}{k}\right)v_{\mathrm{ph}}^2 + 2\hat{C}_{\mathrm{S}}^2\hat{V}_{\mathrm{A}}^4\left(\frac{k_{||}}{k}\right)^3\right\}\mathbf{b}, \\
\mathbf{L} &= \hat{V}_{\mathrm{A}}^2\left\{-(1+\hat{C}_{\mathrm{S}}^2)v_{\mathrm{ph}}^4 + \left[(1+\hat{C}_{\mathrm{S}}^2)\left(\frac{k_{||}}{k}\right)^2 + 2\hat{C}_{\mathrm{S}}^2\right]v_{\mathrm{ph}}^2 - 2\hat{C}_{\mathrm{S}}^2\left(\frac{k_{||}}{k}\right)^2\right\}v_{\mathrm{ph}}^2\mathbf{n} \\
&\quad + \hat{V}_{\mathrm{A}}^2\left\{-\left(\frac{k_{||}}{k}\right)v_{\mathrm{ph}}^4 + (1+\hat{C}_{\mathrm{S}}^2)\left(\frac{k_{||}}{k}\right)v_{\mathrm{ph}}^2 - \hat{C}_{\mathrm{S}}^2\left(\frac{k_{||}}{k}\right)\right\}v_{\mathrm{ph}}^2\mathbf{b}, \\
M &= 3v_{\mathrm{ph}}^5 - 2\left[(1+\hat{C}_{\mathrm{S}}^2)\left(\frac{k_{||}}{k}\right)^2\hat{V}_{\mathrm{A}}^2 + \left(\hat{V}_{\mathrm{A}}^2 + \frac{n_0 h_0}{\mathcal{M}}\hat{C}_{\mathrm{S}}^2\right)\right]v_{\mathrm{ph}}^3 + \left\{\left(\frac{k_{||}}{k}\right)^2\hat{V}_{\mathrm{A}}^2\hat{C}_{\mathrm{S}}^2 + \left[\hat{V}_{\mathrm{A}}^2 + \left(1 + \frac{n_0 h_0}{\mathcal{M}}\right)\hat{C}_{\mathrm{S}}^2\right]\right\}\hat{V}_{\mathrm{A}}^2\left(\frac{k_{||}}{k}\right)^2 v_{\mathrm{ph}}, \\
N &= \hat{V}_{\mathrm{A}}^2\left\{4v_{\mathrm{ph}}^6 - 3\left[1 + \hat{C}_{\mathrm{S}}^2 + \left(\frac{k_{||}}{k}\right)^2\right]v_{\mathrm{ph}}^4 + 2\left[(1+\hat{C}_{\mathrm{S}}^2)\left(\frac{k_{||}}{k}\right)^2 + \hat{C}_{\mathrm{S}}^2\right]v_{\mathrm{ph}}^2 - \hat{C}_{\mathrm{S}}^2\left(\frac{k_{||}}{k}\right)^2\right\}v_{\mathrm{ph}},
\end{aligned} \tag{C2}$$

with $\mathbf{b} = \mathbf{B}_0/B_0$.

[1] J. P. Goedbloed and S. Poedts, *Principles of Magnetohydrodynamics: With Applications to Laboratory and Astrophysical Plasmas* (Cambridge University Press, Cambridge, 2004).
[2] J. P. Goedbloed, R. Keppens, and S. Poedts, *Advanced Magnetohydrodynamics: With Applications to Laboratory and Astrophysical Plasmas* (Cambridge University Press, Cambridge, 2010).
[3] R. Lüst, Fortschr. Phys. **7**, 503 (1959).
[4] M. J. Lighthill, Philosophical Transactions of the Royal Society of London A: Mathematical, Physical and Engineering Sciences **252**, 397 (1960).
[5] K. Kimura and P. Morrison, Phys. Plasmas **21**, 082101 (2014).
[6] M. Lingam, P. Morrison, and E. Tassi, Phys. Lett. A **379**, 570 (2015).
[7] M. Shay, J. Drake, B. Rogers, and R. Denton, J. Geophys. Res. **106**, 3759 (2001).
[8] M. Wardle, Mon. Not. R. Astron. Soc. **307**, 849 (1999).
[9] S. A. Balbus and C. Terquem, Astrophys. J. **552**, 235 (2001).
[10] G. Lesur, M. W. Kunz, and S. Fromang, Astron. Astrophys. **566**, A56 (2014).
[11] P. D. Mininni, D. O. Gómez, and S. M. Mahajan, Astrophys. J. Lett. **567**, L81 (2002).
[12] M. Lingam and S. M. Mahajan, Mon. Not. R. Astron. Soc.: Lett. **449**, L36 (2015).
[13] S. Mahajan and V. Krishan, Mon. Not. R. Astron. Soc.: Lett. **359**, L27 (2005).
[14] M. Lingam and A. Bhattacharjee, Astrophys. J. **829**, 51 (2016).
[15] S. M. Mahajan and Z. Yoshida, Phys. Rev. Lett. **81**, 4863 (1998).
[16] E. Hameiri and R. Torasso, Phys. Plasmas **11**, 4934 (2004).
[17] A. Lichnerowicz, S. C. for Advanced Studies, and T. M. P. M. Series, *Relativistic Hydrodynamics and Magnetohydrodynamics*, Vol. 35 (WA Benjamin, New York, 1967).
[18] A. M. Anile, *Relativistic Fluids and Magneto-Fluids* (Cambridge University Press, Cambridge, 1990).

[19] S. Koide, Astrophys. J. **696**, 2220 (2009).
[20] S. Koide, Astrophys. J. **708**, 1459 (2010).
[21] L. Comisso and F. A. Asenjo, Phys. Rev. Lett. **113**, 045001 (2014).
[22] F. A. Asenjo and L. Comisso, Phys. Rev. Lett. **114**, 115003 (2015).
[23] F. A. Asenjo, L. Comisso, and S. M. Mahajan, Phys. Plasmas **22**, 122109 (2015).
[24] Y. Kawazura, G. Miloshevich, and P. J. Morrison, Phys. Plasmas **24**, 022103 (2017).
[25] E. Hameiri, A. Ishizawa, and A. Ishida, Phys. Plasmas **12**, 072109 (2005).
[26] G. Kalra and W. Gebretsadkan, Phys. Plasmas **7**, 3531 (2000).
[27] R. Keppens and Z. Meliani, Phys. Plasmas **15**, 102103 (2008).
[28] A. R. Soto-Chavez, S. M. Mahajan, and R. D. Hazeltine, Phys. Rev. E **81**, 026403 (2010).
[29] F. A. Asenjo, V. Muñoz, J. A. Valdivia, and T. Hada, Phys. Plasmas **16**, 122108 (2009).
[30] V. Muñoz, F. A. Asenjo, M. Domínguez, R. A. López, J. A. Valdivia, A. Viñas, and T. Hada, Nonlinear Processes in Geophysics **21**, 217 (2014).
[31] $T_e/m_e c^2 \lesssim 1$ is a rather restrictive condition for actual relativistic astrophysical objects, and the electron thermal inertia is effective even in ion inertial length as we pointed out in the past study [24]. However, we assume $T_e/m_e c^2 \lesssim 1$ to single out the role of the Hall effect. We may superpose the electron thermal inertia effect to Hall effect in the linear wave property. The study on the electron thermal inertia effect will be a future work .
[32] A. Taub, Phys. Rev. **74**, 328 (1948).
[33] S. M. Mahajan, Phys. Plasmas **23**, 112104 (2016).
[34] A. Ito, A. Hirose, S. M. Mahajan, and S. Ohsaki, Phys. Plasmas **11**, 5643 (2004).
[35] A. Hirose, A. Ito, S. M. Mahajan, and S. Ohsaki, Phys. Lett. A **330**, 474 (2004).
[36] J. J. Barnard and J. Arons, Astrophys. J. **302**, 138 (1986).
[37] M. Lyutikov, Mon. Not. R. Astron. Soc. **293**, 447 (1998).
[38] B. Zhang and H. Yan, Astrophys. J. **726**, 90 (2010).